Child Neurology Open
1-10

DOI: 10.1177/2329048X211034969
journals.sagepub.com/home/cno
SAGE

Tubulin Folding Cofactor D Deficiency: Missing the Diagnosis With Whole Exome Sequencing

Christina M. Quitmann[1], Stephan Rust, Dr. rer. nat.[1], Janine Reunert, Dr.[1], Saskia Biskup, Dr. med. Dr. rer. nat.[2], Barbara Fiedler, Dr. med.[1], and Thorsten Marquardt, Dr. med.[1]

Abstract

Two siblings with an early onset of a neurodegenerative disease were presented with muscular hypotonia, secondary microcephaly, and severe developmental delay. Seizures were refractory to treatment but could be controlled with a ketogenic diet. Over the course of 5 years, whole exome sequencing (WES) was performed twice in both children. The first time the diagnosis was missed. The next one revealed compound heterozygous mutations in the gene coding for the tubulin folding cofactor D. Technical improvements in WES mandated a new investigation after a few years in children where the diagnosis has not been found.

Keywords

TBCD deficiency, tubulin, ketogenic diet, neutropenia, whole exome sequencing

Received March 3, 2021. Received revised June 18, 2021. Accepted for publication July 7, 2021.

Introduction

Microtubules play a crucial role for the cytoskeleton and are essential to develop synaptic connections, as well as to build axons and dendrites. They consist of α- and β-tubulins that form heterodimers and subsequently protofilaments. Several protofilaments build a hollow tubular structure. Polymerization and depolymerization of the microtubules are essential in proliferation, communication, development, and motility, which are organized by microtubule-organizing centers (MTOCs). To settle the polarity of the microtubules, a γ-tubulin ring complex is crucial because it functions as a microtubule nucleator at the MTOC and binds the β-subunit to expose the α-subunit (Zheng et al[1]).

The correct building of microtubule blocks requires additional proteins and cofactors. Native α- and β-tubulins initially interact with prefoldin, which is responsible for bringing them together with their corresponding chaperonin (chaperonin containing TCP-1 [CCT]—cytosolic chaperonin) (Vainberg et al[2]). After adenosine triphosphate hydrolysis, α- and β-tubulins interact with specialized chaperons, the tubulin folding cofactors, which assist in the correct folding of the α/β-tubulin heterodimers. Tubulin folding cofactor A (TBCA) is part of the β-folding pathway and tubulin folding cofactor B (TBCB) is part of the α-folding pathway. Tubulin folding cofactor C (TBCC), tubulin folding cofactor D (TBCD), and tubulin folding cofactor E (TBCE) are involved in both pathways. TBCB and TBCA need to bind to native α- and β-tubulins before the following cofactors can build a complex. Cofactors D, E, and C build the super complex with α- and β-tubulin to hydrolyze guanosine triphosphate (GTP). This results in the release of the correctly folded native α- and β-tubulin (see Figure 1). α- and β-tubulin monomers from depolymerized microtubules may also be recycled into this pathway by direct binding to TBCE and TBCD, respectively (see dotted dash line arrows in Figure 1) (Lewis et al[3]). ARL2, an adenosine diphosphate

[1]University Children's Hospital Muenster, Muenster, Germany
[2]Center for Genomics and Transcriptomics, Tübingen, Germany

Corresponding Author:
Christina M. Quitmann, Department of General Pediatrics, Metabolic Diseases, University Children's Hospital Muenster, Albert-Schweitzer-Campus 1, 48149 Muenster, Germany.
Email: c_quit01@uni-muenster.de

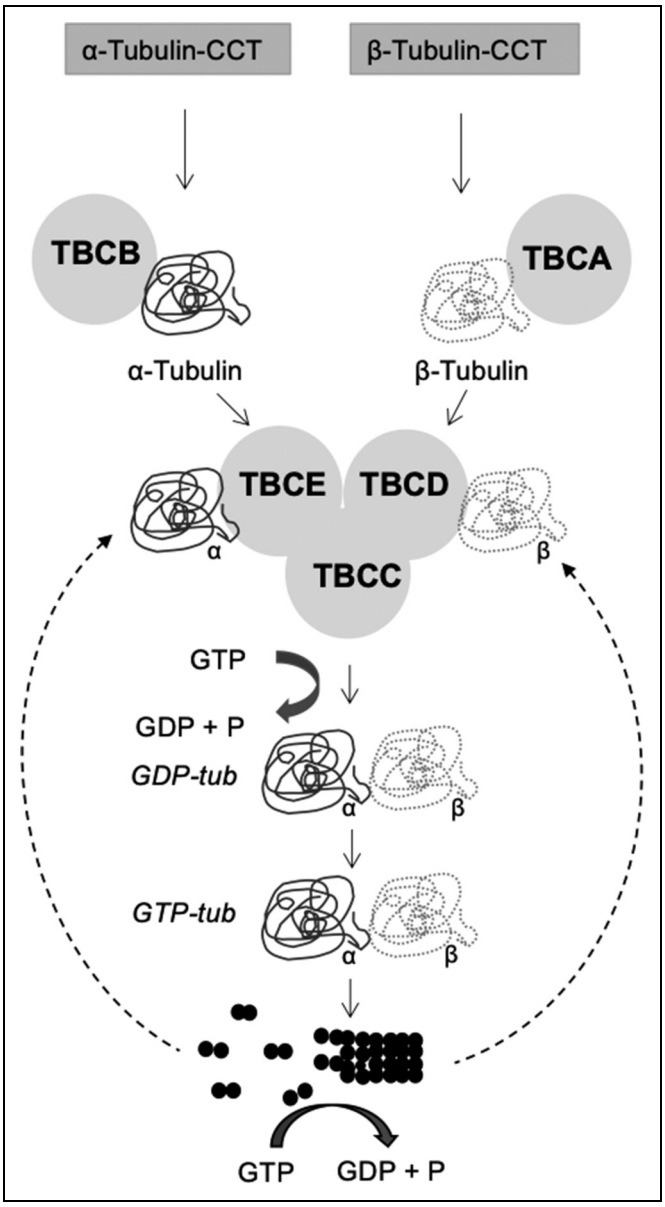

Figure 1. (CCT) This picture shows the tubulin folding pathway and the involvement of several cofactors. The microtubules depolymerization depends on GTP hydrolysis and the correct interaction with the cofactors. TBCA and TBCB are described exclusively in 1 pathway, whereas TBCC, TBCD, and TBCE build the super complex to hydrolyze GTP and facilitate the release of the native tubulins. TBCD is crucial to release the native β-tubulin (modified from Bhamidipati et al[5]).
Abbreviations: CCT, chaperonin containing TCP-1; GTP, guanosine triphosphate; TBCA, tubulin folding cofactor A; TBCB, tubulin folding cofactor B; TBCC, tubulin folding cofactor C; TBCD, tubulin folding cofactor D; TBCE, tubulin folding cofactor E.

ribosylation factor-like protein, is involved in the regulation of the folding pathway by interacting with TBCD and β-tubulin. The TBCD·ARL2·β-tubulin trimer is a functional complex whose role is crucial in microtubule assembly (Francis et al[4]).

Several neurodegenerative diseases are described in the literature that have their cause in mutations of proteins, which are involved in microtubule formation or posttranslational modifications[6] (MIM: #617193). Mutations in TBCD can result in a defective function of the cofactor and deficiencies in the structure, folding, or stability of the microtubules[7] (Flex et al[8]) and lead to neuronal degenerative disorders (Miyake et al[9]).

Whole exome sequencing (WES) is a very powerful method to diagnose ultra-rare genetic disorders such as TBCD deficiency. Often, it is only done once and not repeated even if no diagnosis could be found. However, continuous improvement of the method suggests that it can be useful to repeat the analysis.

Materials and Methods

Array-comparative genomic hybridization (CGH) was performed in February 2010 using an Agilent 400k Array. Single nucleotide polymorphism (SNP)-chip analyses for homozygosity and identical by descent mapping were done essentially as described in Tegtmeyer et al[10] using Illumina 660 W beadchips. The logarithm of the odds scores over the chromosomes were calculated using Merlin-1.1.2 software.[11] Two exome analyses were done by CEGAT (Tübingen). For the first exomes in 2013, enrichment of exonic sequences was achieved with the Agilent Exome v.5 kit. For sequencing, an Illumina HiSeq2500 was used. For each patient, data from two runs were pooled. Reads were mapped to the *hg*19 reference sequence using the bwa-tool 0.7.2-r351. Variants were called with samtools 0.1.18 + bcftools 0.1.17 and VarScan 2.3.5. Annotation was based on Ensembl.74 + RefSeq.UCSC.20131210 + CCDSr15, dbSNP 138, dbNSFP 2.1, exome variant server , and human gene mutation database (HGMD) version 2013.04. Regarding the new exomes in 2018, enrichment was by Agilent Exome v.7, adapter trimming by Skewer 0.2.2 software, mapping to *hg*19 reference sequence using the bwa-tool 0.7.2-r351, variant calling by CeGaT StrataCall r1254, annotation was based on Ensembl.75 + RefSeq.UCSC.20180712 + CCDSr15, dbSNP 151, dbNSFP 3.4c, GnomAD 2.0.2, HGMD 2018.02, and indel realignment by assembly based realigner (PMID: 24907369).[11]

To investigate the effect of the discovered mutations in the TBCD gene (RefSeq GenBank: NM_005993.5), complementary DNA (cDNA) was synthesized using RNA obtained from peripheral blood cells by standard procedures. The region of interest was amplified using primers in exons 20 and 28 (5′- GAGGCTGCTGTCCATGACACTGAG, 5′-GGGGAAG TGTGGGTAACTGCTCT, product length 606 bp). Primers were 5′-tailed with M13 forward and reverse adapters for simplified sequencing M13F: TGTAAAACGACGGCCAGT and M13R: CAGGAAACAGCTATGACC. The product was sequenced by standard Sanger sequencing, using BigDye-terminator technology and primers M13F and M13R. Primers were searched using Primer blast software[12] against sequences of the respective exons with neighboring intron regions. These sequences were extracted from Ensembl, ENSG00000141556.

Results

Two siblings with a neurodegenerative disease are described with epileptic seizures, secondary microcephaly, and a severe developmental delay. Both siblings carry heterozygous, disease-causing mutations in the TBCD gene.

Patients

The two siblings descent from healthy, unrelated parents who did not report any inherited disease in their family. Informed consent was obtained from the parents.

Patient A (female) was born 3 weeks prior to the estimated date of birth with a body weight of 3140 g (36th percentile), length of 51 cm (48th percentile), 33.5 cm head circumference (24th percentile), Apgar 09/10/10, and umbilical cord pH (A) 7.3. She was presented at our hospital at the age of 8 months due to seizures and developmental delay. During the seizures, she grimaced and gazed at the top right. She showed hypersalivation and a fencing posture. The seizures were initially fever-associated but later occurred unprovoked. In the first clinical examination, she showed few spontaneous movements and could not sit without support. She presented with a progressive hypotonia of the lower limb that had been noticed before in a routine screening at the age of 6 months. She had a secondary microcephaly as well as a marginal splenomegaly with 7.5 cm (normal: <7.2 cm). No cardiac, abdominal, or pulmonic abnormalities were observed at this point of the investigation. She developed talipes equinus on both sides and hip luxations. Her length and weight were within the 25th and 50th percentile but her head circumference was below the third percentile. The newborn screening for metabolic disorders and the blood amino acids were normal. During the first 9 months, methylmalonic acid in the organic acids was several times significantly elevated and declined after the administration of vitamin B_{12}.

The first electroencephalogram (EEG) was pathological with beta activity overlay and epileptiform discharges on the right hemisphere. Physiological stages of sleep were not verifiable. The following EEGs showed sharp-wave complexes on the left and right hemispheres. Tachycardia and low oxygen saturation were part of the seizures and generally higher amplitude on the right hemisphere was noticed. The patient slept a lot and regularly showed small seizures after waking up during the day. The seizures were both myoclonic and tonic and occurred with screaming or laughing.

Several anticonvulsive drugs were used in mono and combination therapy (eg sulthiame, oxcarbazepine, topiramate, ethosuximide, and levetiracetam) led to fewer seizures, however, episodes with atypical absences remained. Finally, the patient was free from seizures after a ketogenic diet was introduced (see Figure 2).

Brain magnetic resonance imaging (MRI) revealed reduced supratentorial white matter volume and a hypoplasia of the corpus callosum. The neurocranium and myelination were age-appropriate at 8 months; however, a lack of developmental progression of myelinization in the following MRI was observed. Progressive brain atrophy with consecutive hydrocephalus ex vacuo was seen in the subsequent MRIs. Brain atrophy affected gray and white matter equally including the basal ganglia. The head of the caudate nucleus was almost undetectable in the MRI (see Figure 3).

Motor nerve conduction velocity was significantly reduced since the patient's first presentation at the age of 8 months (nervus tibialis posterior and nervus ulnaris). No signs of

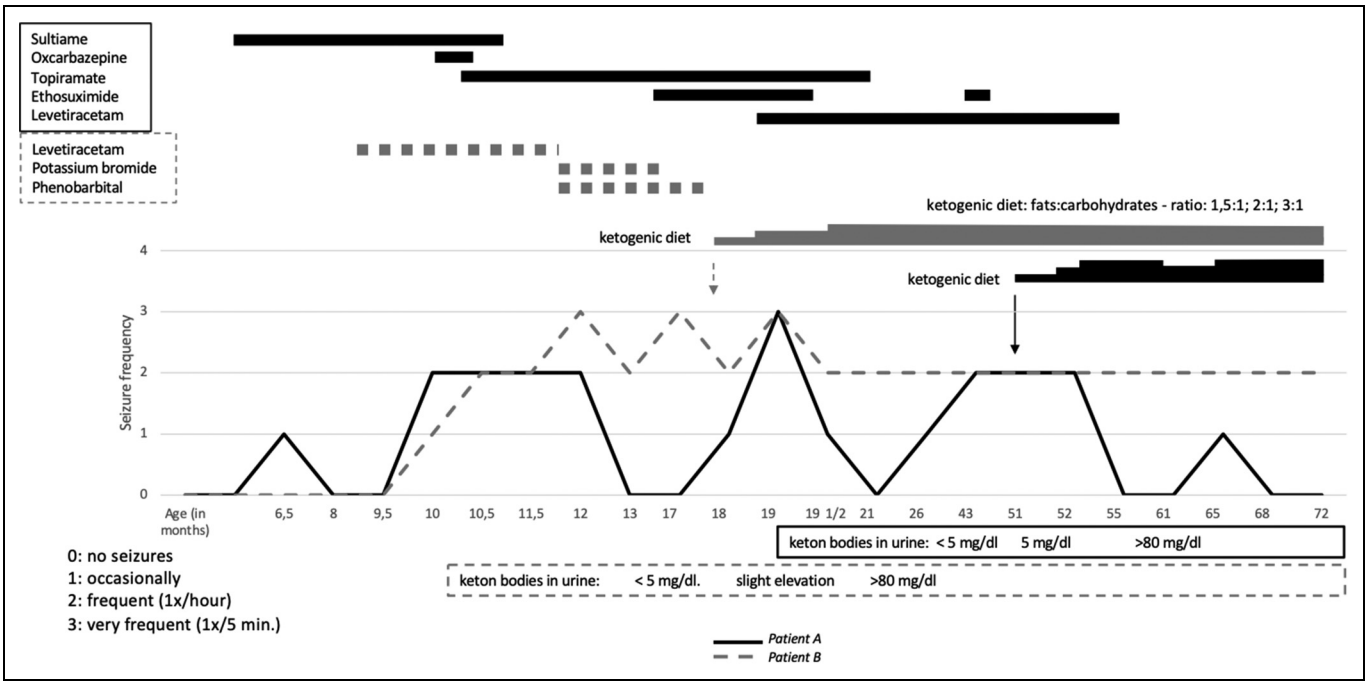

Figure 2. Seizure frequency under anticonvulsive therapy and ketogenic diet in patients A and B.

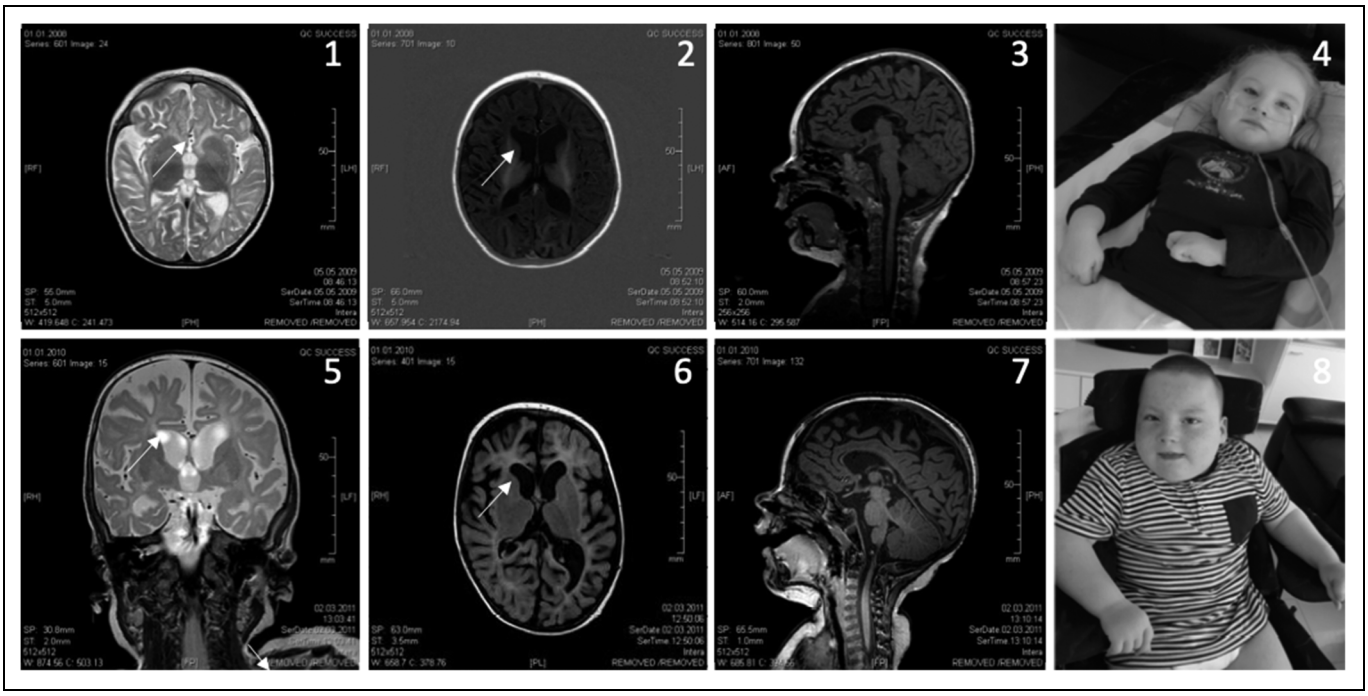

Figure 3. Patient A (1-3): Magnetic resonance imaging at the age of 12 months with progressive loss of brain volume. Extended liquor ventricles, hypomyelination and progressive depletion of the corpus callosum, and an almost nondefinable head of caudate nucleus (arrow) were observed. The photograph (4) was taken at the age of 7 years. Patient B (5-7), Magnetic resonance imaging at the age of 11 months showing a distinct global brain atrophy, hypomyelination and a thin corpus callosum. Especially the hippocampal regions and the caudate nuclei are thinned out (arrow). The photograph (8) was taken at the age of 8 years.

inflammation were observed in the muscle biopsy, but a pattern of neurogenic damage with fiber atrophy and hypertrophic groups of fibers was found. Sural nerve biopsy was normal. Her patellar, Achilles tendon, biceps, and triceps tendon reflexes were present until the age of 2.5 years. At this point exclusively the pupillary light reflex was consistently noticeable. She expressed almost no control over her head movements and developed a heavy tremor. She showed little motoric development but was able to express emotions such as joy and pain.

At 19 months of age, a premature thelarche was reported. Her breast development was classified according to the Tanner System as PH 1 B3. Furthermore, she had a growth spurt without a puberty-typical hormone profile or bone age, which made a precocious puberty seem unlikely. Due to muscular hypotension, she suffered from dysphagia and recurrent pulmonary infections. Furthermore, she developed an elevated diaphragm and atelectasis, which was treated symptomatically. Both patients developed intermittent neutropenia in the first years of life.

She had not reached the development milestones appropriate for her age from the age of 7 months onward, but she even lost previously acquired capabilities. At the age of 10 months, she could control her head occasionally, but she could not roll from front to back on her own, neither could she sit freely. Her grasp was uncoordinated, but she could laugh, focus, babble unspecifically, and show emotions.

She died at the age of 7 years of an airway infection.

Her younger brother, patient B, was born 2 weeks prior to the estimated date of birth with a body weight of 3420 g (52nd percentile), length of 50 cm (26th percentile), head circumference of 35 cm (52nd percentile), Apgar 09/10/10, and umbilical cord pH (A) 7.3. He had developed completely appropriate to his age in the first 3 months after birth. Then he started to move less and showed extension in the legs while lifting him. At the age of 6 months, he presented with a hypotonia of the lower limb after kicking and moving actively in the first months after birth. He showed progressive hypotonia, neurodevelopmental delay, and fever associated epileptic seizures. In the first examination, the muscular reflexes were still present. By 9 months he stopped turning on the sides. He was diagnosed with a massive psychomotor retardation.

The EEG showed an asymmetry between the right and the left hemisphere. Sharp waves and beta activity overlay were observed. A treatment with levetiracetam did not decrease the seizure frequency, and he stayed very tired during the day. By 12 months he presented with fever while seizures appeared every 3 min. The anticonvulsive therapy was optimized with phenobarbital, which could decrease the seizure frequency to once every 20 to 60 min. Potassium bromide was added on suspicion of migrating partial epilepsy but needed to be stopped because of side effects. The seizure frequency remained high during occasionally occurring fever episodes. Eventually, a ketogenic diet finally decreased the seizure frequency with a fat–carbohydrate ratio of 3:1. The ketone bodies in the urine exceeded 80 mg/dL (see Figure 2).

During the day, he still had several myoclonic twitches lifting his arms and opening his eyes wide. Occasionally he

expressed a fencing posture. The pattern of myoclonia presented identically compared with the sister's myoclonia. No physiological sleep structures appeared in the EEG, and he maintained a high susceptibility to seizures. The MRI results of both siblings showed similarities (see Figure 3). He developed dysphagia and from the age of 2.5 years, he received a majority of his food via a percutaneous endoscopic gastrostomy tube. He did not develop any ability to speak, had convergent strabism, and at 9 years old he developed nystagmus. The parents reported that the hand-mouth-contact had stopped by 5 years, and by 7 years he showed significantly less movement and anticipation. He is now 10 years old.

Retrospectively, the mother reports several differences among the pregnancies with the 2 affected children and the following healthy sibling. The affected pregnancies shared a cervix insufficiency, which required a cervical cerclage; increased heart rates of the fetuses at around 160/170 bpm; and significantly less movement and activity. An ultrasound in the 20th week already showed borderline abnormalities in the brain, and both affected children were born 3 weeks early due to premature contractions.

Genetics

The chromosomal analysis showed a standard karyotype and array CGH was inconspicuous. Since the parents came from a limited population of German immigrants to Russia, we also checked for unknown consanguinity by SNP-chip-analysis. In total 13.7 Mb of the genome were shared homozygous by the siblings, but WES showed no relevant mutations in those regions. About one-third of the genome was shared identical by descent by the siblings, but using the results of the first exome analysis no compound heterozygous mutations led to a candidate gene. The average coverage of that exome was 144× with 96.2% at least 30× for patient A and 308× with 98.7% at least 30× for patient B. The second exome in 2018 revealed 2 mutations in TBCD in both siblings (see Table 1). Retrospective inspection of the 2013 data showed that the c.230A > G was contained in the variant lists of both siblings, but the gene did not appear as relevant since the second mutation was not covered sufficiently (see Table 1, numbers taken from mapping-file), was therefore filtered off and was not listed in the respective variant list of patient A.

Furthermore, no disease-causing mutation had been identified and published until 2016. The WES in 2018 (average coverage 149×; 96.7% at least 30× for patient B) finally led to our diagnosis and located the compound heterozygous mutation in patient B (see Table 1). Because patient A had been deceased just the correspondent regions were mapped again. The variant c.2048_2052dupTAATA; p.Glu685* was confirmed with Sanger sequencing because 2 reads of the variant with next generation sequencing were not sufficient.

By WES, the compound heterozygous mutations c.230A > G and *c.2048_2052dup* in the gene coding for TBCD were found in both patients. The mother is a heterozygous carrier of the missense mutation. The father is a heterozygous carrier of the variant *c.2048_2052dup* TAATA; p.Glu685* in exon 24, which results in a premature stop codon and probably in the following to a nonsense-mediated messenger RNA decay. This could clearly be visualized by a significantly reduced signal of the affected allele in the cDNA (panel B) in comparison with wild type cDNA (panel A) (see Figure 4).

The variant c.230A > G is predicted to be "deleterious" by PROVEAN,[13] "likely pathogenic" by ClinVar (submitted 2018, submission number: SCV000892499)[14] and "damaging" by sorting intolerant from tolerant (SIFT).[15] Furthermore, both variants are predicted to be "disease causing" by mutation taster.[16] In the following, we present a table with the known disease-causing mutations and references leading to a similar clinical presentation (see Table 2).

Discussion

We presented two patients with a severe neurodegenerative disease with 1 novel mutation in the TBCD gene and a particularly severe clinical phenotype.

The laboratory findings showed in both patients intermittent neutropenia. A possible explanation for the neutropenia could be the enhanced stability of the microtubules in TBCD deficiency, which was investigated and determined by Flex et al.[8] This has also been observed as a side effect of the drug taxol. Taxol stabilizes microtubules (Abal et al[27]) and often leads to neutropenia (Rowinsky et al[28]).

We contemplate a hormonal involvement of the disease because our female patient presented with premature thelarche at the age of 19 months. A TBCD-deficient patient with hirsutism had been described in the literature,[26] as well as a patient with cryptorchidism and hypothyroidism.[18] Moreover, our male patient had undescended testicles, which could be caused by multiple factors. Further investigation of TBCD deficiency would be necessary to clarify a hormonal interaction of the disease.

Table 1. The Coverage of the Correspondent Regions in Whole Exome Sequencing (Patient A Female, Patient B Male); Given are the Counts Normal/Mutant Allele.

	Patient A		Patient B	
	c.230A > G	c.2048_2052dupTAATA; p.Glu685*	c.230A > G	c.2048_2052dupTAATA; p.Glu685*
2013 (CeGaT)	19/22	2/1 + 1 other divergent read at this position	27/23	8/3 + 1 other divergent read at this position
2018 (CeGaT)	53/57	6/2	129/136	30/19

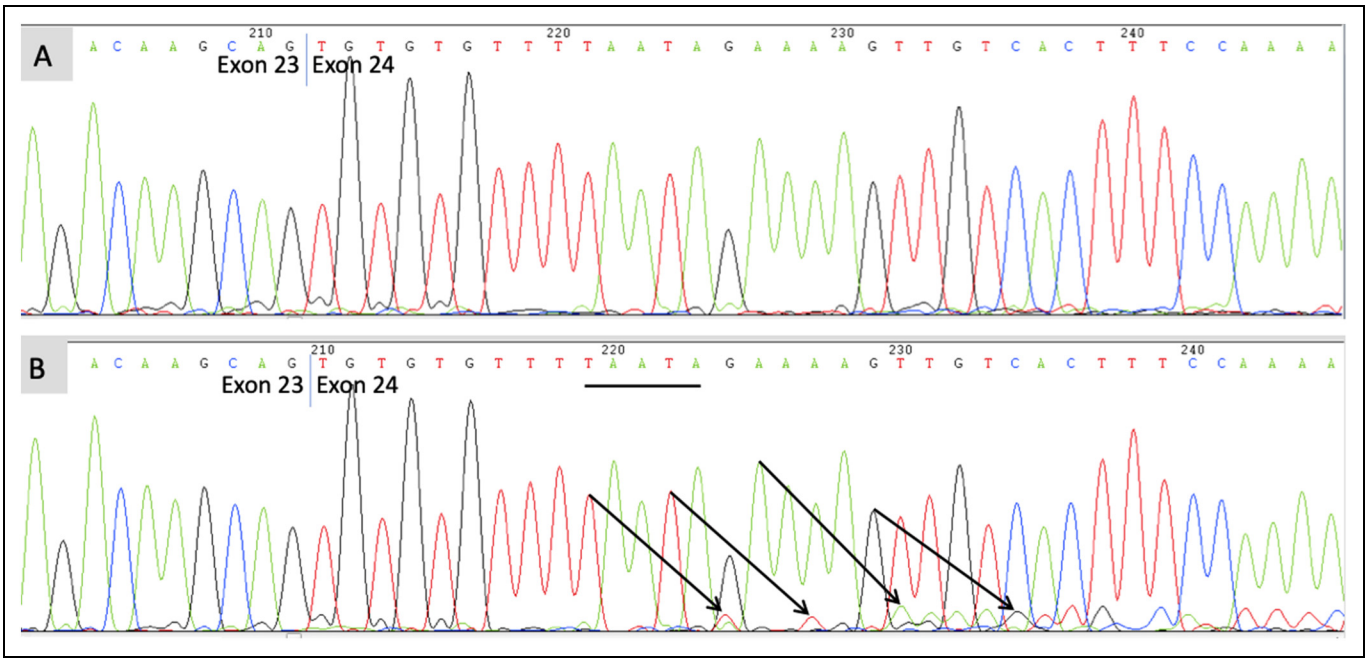

Figure 4. (A) Shows a healthy control, whereas the sequencing of exon 24 in the patient's complementary DNA. (B) Shows a decreased signal in the region of the duplicated TAATA-sequence (underlined).

By reconstructing the diagnostic way of the 2 patients, we want to emphasize the importance of reevaluation and potential repetition of diagnostics, especially if new technology is available. The average coverage had improved remarkably while the amount of required material decreased in the last decade which allows us to analyze more samples per run. The percentage of target sequences covered at least 20-fold had increased just marginally from ~97% to 98% in the time between the first and the last successful sequencing. This overall improvement, however, also included significant relative improvements of many outliers (see Figure 5).

Additionally, we can report a novel disease-causing mutation (c.2048_2052dupTAATA; p.Glu685*) that had not been described previously. The heterozygous mutation c.230A > G had been described by Tian et al[19] with a mild clinical manifestation. The variant c.230A > G in combination with the deletions of exons 28-39 leads to a heavy clinical manifestation with a phenotype similar to our patients (Zhang et al[17]), as well as the homozygous mutation (Elmas et al[18]). We compare the clinical presentation of the patients carrying the same variant c.230A > G in Table 3.

The characteristics of phenotypes most likely depend on the remaining protein function and especially on the ability to interact with the cofactors and β-tubulin(Miyake et al[9]).

The milder mutation in our case might be the missense mutation *c.230A > G* and determines the clinical picture. It remains unclear whether modulating factors are present in the different patients.

At first glance, the second TBCD allele does not explain the clinical difference, as in all 3 cases a loss of function is predicted. A dominant effect, eg by incorporation of some truncated nonfunctional forms into the DEα-/β-tubulin/C-super complex, is also unlikely, since the parents were completely normal. However, it cannot be excluded that the mutation c.907C > T (p.Arg303*) reported by Tian et al[19] is a hypomorphic nonsense mutation providing a relevant residual function. This may occur through mutation-induced alternative splicing with new splice sites or by exon skipping, leaving a protein with a significant remaining function (eg Roosing et al[29]) or by a significant percentage of read through. This could solve the paradox. In the patient described by Tian et al,[19] the mutation c.230A > G would be the more severe defect than the hypomorphic stop, which would explain the mild phenotype in their patient(s) (Table 3). In contrast, the other patients in Table 3 with the heterozygous mutation likely would have a true stop as the second allele explaining their more severe phenotype. The homozygous missense mutation also leads to a severe phenotype because the residual protein function does not suffice.

The patient's complete genetic background should not be overlooked and be considered as a significant influence on the manifestation of the disease.

Forty-three patients with various mutations in the TBCD gene but different phenotypes had been described so far. The majority of patients developed a severe neurodegenerative disorder with an early onset within the first year; very few patients with mild clinical features could be identified. Aside from a symptomatic antiepileptic pharmacotherapy, there is no causal treatment until now. Most of the children developed severe respiratory problems and deceased within months or a few years.

The disease is probably underdiagnosed and not very widely known. It took a long time until the children could be diagnosed correctly. Early WESs did not result in the correct diagnosis, mostly due to a low coverage in the correspondent regions. The first description of the disease had not been published at

Table 2. Known Disease-Causing Mutations in Tubulin Folding Cofactor D.

Nucleotide mutation (+1 as A of ATG start codon)	Consequence of mutation	Annotation	Reference	Clinical comparator
c.2048_2052dupTAATA; p.Glu685* (het.)	p.Glu685*→stopgain	rs1568044300	This study	
c.230A > G (het.)	p.His77Arg	rs1409600874	This study, Zhang et al[17]	
deletion of exons 28-39 (het.)			Zhang et al[17]	
c.230A > G (hom.)	p.His77Arg		Elmas et al[18]	Onset: 5 months, severe delay, spastic tetraplegia, seizures, brain atrophy
c.3365C > T (het.)	p.Pro1122Leu	–	Tian et al[19]	
c.1739G > A (het.)	p.Arg580Gln	–		
c.230A > G (het.) c.907C > T (het.)	p.His77Arg p.Arg303*→stopgain	rs751190601		
c.2953*C* > *T* (het.)	p.Arg979Cys	rs768723646		
c.3550C > T (het.)	p.Gln1184*→stopgain	rs754168355		
c.2419G > A (het.)	p.Glu807Lys	rs199644299	Di Bella et al[20]	
c.2852 + 3A > G (het.)		rs187081192		
c.202C > T (het.)	p.Gln68Ter	–	Isik et al[21]	
c.880C > T (het.)	p.Arg294Trp	rs200591137		
c.1423G > A (het.) c.554del (het.)	p.Ala475Thr p.Lys185Argfs*14	– –	Stephen et al[22]	
c.(3099C > G) (hom.)	p.Asn1033Lys	–	Gronborg et al[23]	Onset: 4–9 months, developmental regression, secondary microcephalus, hypotonia, spasticity, and early death
c.2825G > A (hom.)	p.Arg942Gln	rs1056577423	Ikeda et al[24]	Onset: 1/6 month(s), Severe phenotype, epilepsy, early need of ventilation, and severe retardation
c.1423G > A (hom.)	p.Ala475Thr	–	Pode-Shakked et al[25]	Secondary microcephalus, epilepsy, hypotonia, intellectual disability, and mild dilatation of the ventricles
c.2810C > G (hom.)	p.Pro937Arg	–		Mild ataxia, secondary microcephalus, epilepsy, intellectual disability, and mild cortical atrophy
c.1757C > T (het.)	p.Ala586V	–		
c.3192-2A > G (het.)	IVS34-2A > G	–		
c.1160T > G (het.)	p.Met387Arg	–	Miyake et al[9]	
c.1564-12C > G (het.)	p.Gly522Phefs*14	–		
c.2280C > A (het.)	p.Tyr760*	–		
c.2314C > T (het.)	p.Arg772Cys	rs181969865		
c.2761G > A (het.)	p.Ala921Thr	rs886041085		
c.2810C > G (hom)	p.Pro937Arg	–		Onset: 9/11 months, epilepsy, regression, microcephalus, hypotonia, and muscle atrophy
c.3365C > T (hom)	p.Pro1122Leu	rs755177846	Flex et al[8]	Severe manifestation
c.2981C > T (het.)	p.Thr994Met	rs867484272		
c.3313G > A (het.)	p.Val1105Met	rs764003906		
c.1876G > A (het.)	p.Ala626Thr	rs749225304		
c.1130G > A (het.)	p.Arg377Gln	rs764085684		
c.771 + 1_771 + 10del (het.)		rs1408793828		
c.1121C > T (het.)	p.Thr374Met	–		
c.686T > G (het.) c.3365C > T (het.)	p.Leu229Arg p.Pro1122Leu	rs778417127 rs755177846		
c.1423G > A (hom.)	p.Ala475Thr	–	Edvardson et al[26]	Onset: 10/14 months, severe epilepsy, dystonia, and nystagmus
c.1757C > T (hom.)	p.Ala586Val	–		Onset: 12 months, rare epilepsy, dystonia, and spasticity

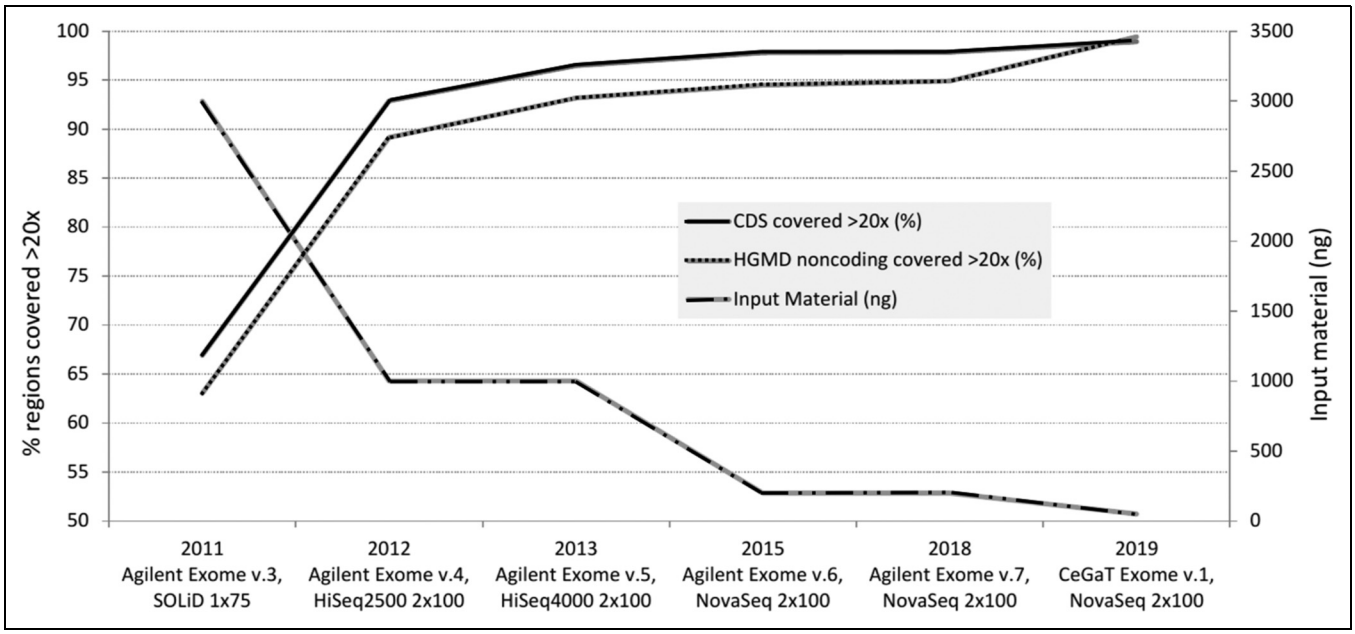

Figure 5. This chart illustrates the increase of covered regions exceeding 20-fold with WES (CDS, and HGMD). The higher the coverage of coding sequences and disease-causing genes documented by the HGMD, the higher the probability to identify rare disease-causing mutations and interpret them correctly. While the coverage improved immensely in the last decade, the required input material decreased due to technological advance (CeGaT). The combined effect of the determinants facilitated diagnosing the TBCD deficiency.
Abbreviations: WES, whole exome sequencing; CDS, coding sequences; HGMD, human gene mutation database; TBCD, tubulin folding cofactor D.

Table 3. Comparison of Patients From Studies of Tian et al[19] and Zhang et al[17] Carrying the Same Heterozygous Variant With Different Phenotypes (N/A: Not Applicable).

	c.230A > G; c.907C > T[19] ($n = 1$)	c.230A > G; deletions of exons 28–39[17] ($n = 1$)	c.230A > G; c.2048_2052dupTAATA ($n = 2$)	c.230A > G c.230A > G ($n = 1$)[18]
Seizures	Fever associated and good response to epileptic drugs	Not fever associated, refractory to epileptic drugs	Fever associated and refractory to epileptic drugs, ketogenic diet reduced seizures	Present
Age of onset	6 months	9 months	6 months (patient B) 8 months (patient A)	5 months
EEG	Low amplitude spike waves midline, bilateral central top and frontal region during sleep	High amplitude delta wave, during the seizures migration between both hemispheres	Asymmetry between the right and the left hemisphere. Sharp waves and beta activity overlay.	N/A
MRI	Myelination delay and defect in the white matter of the occipital lobe	Atrophy, thin corpus callosum, extended liquor ventricles, and hypomyelination	Atrophy, thin corpus callosum, extended liquor ventricles, hypomyelination, and undefinable head of caudate nucleus	Bifrontotemporal atrophy, dilated bilateral ventricles and third ventricular, periventricular hyperintensity, and thin corpus callosum
Neurological examen	Nearly normal	Severe delay	Severe delay	Severe delay
Secondary microcephalus	No	Yes (<3 percentile)	Yes (<3 percentile)	N/A
Milestones	Almost reached the milestones according to the age	Developmental regression after the onset	Developmental regression after the onset	Severe delay
Hypotonia	No	Yes	Yes	N/A

Abbreviations: EEG, electroencephalogram; MRI, magnetic resonance imaging.

that point. WES experienced a rapid development in the last decade due to the introduction of new diagnostic tools and efforts to increase efficiency. This progress was accompanied by an improvement of the coverage, which is an essential marker for the quality of a sample (Matthijs et al[30]). Overall, this advance and the publications about the candidate gene were crucial for the diagnosis of the patients presented above.

The current WES has a better coverage and makes faster diagnosis possible. In general, unresolved cases may profit from the repetition of sequencing using improved processes that facilitate the identification of rare diseases and may therefore provide the basis for any development of a specific therapeutic approach.

Acknowledgments

The work was performed in the University Children's Hospital in Muenster, Germany.

Author Contributions

Christina M Quitmann drafted the manuscript and contributed to analysis and interpretation of data. A substantial contribution to the analysis and interpretation of data was made by Stephan Rust, Dr. rer. nat. and Janine Reunert, Dr. Biskup Dr. rer. nat., Dr. med. and Barbara Fiedler Dr. med. contributed to acquisition of data and interpretation. Thorsten Marquardt Prof., Dr. med. supervised the work and contributed to conception and interpretation of the data. All authors had critically revised the manuscript, finally approved it and agree to be accountable for all aspects of the work.

Declaration of Conflicting Interests

The authors declared no potential conflicts of interest with respect to the research, authorship, and/or publication of this article.

Funding

The authors received no financial support for the research, authorship, and/or publication of this article.

ORCID iD

Christina M. Quitmann https://orcid.org/0000-0001-8759-1613

Ethical Approval

Not applicable, because this article does not contain any studies with human or animal subjects.

References

1. Zheng Y, Wong ML, Alberts B, Mitchison T. Nucleation of microtubule assembly by a gamma-tubulin-containing ring complex. *Nature*. 1995;378(6557):578-583. doi:10.1038/378578a0
2. Vainberg IE, Lewis SA, Rommelaere H, et al. Prefoldin, a chaperone that delivers unfolded proteins to cytosolic chaperonin. *Cell*. 1998;93(5):863-873. doi:10.1016/s0092-8674(00)81446-4
3. Lewis JA, Tian G, Cowan NJ. The alpha- and beta-tubulin folding pathways. *Trends Cell Biol*. 1997;7(12):479-484.
4. Francis JW, Newman LE, Cunningham LA, Kahn RA. A trimer consisting of the tubulin-specific chaperone D (TBCD), regulatory GTPase ARL2, and beta-tubulin is required for maintaining the microtubule network. *J Biol Chem*. 2017;292(10):4336-4349. doi:10.1074/jbc.M116.770909
5. Bhamidipati A, Lewis SA, Cowan NJ. ADP ribosylation factor-like protein 2 (Arl2) regulates the interaction of tubulin-folding cofactor D with native tubulin. *J Cell Biol*. 2000;149(5):1087-1096. doi:10.1083/jcb.149.5.1087
6. Baird FJ, Bennett CL. Microtubule defects & neurodegeneration. *J Genet Syndr Gene Ther*. 2013;4:203. doi:10.4172/2157-7412.1000203
7. Cunningham LA, Kahn RA. Cofactor D functions as a centrosomal protein and is required for the recruitment of the gamma-tubulin ring complex at centrosomes and organization of the mitotic spindle. *J Biol Chem*. 2008;283(11):7155-7165. doi:10.1074/jbc.M706753200
8. Flex E, Niceta M, Cecchetti S, et al. Biallelic mutations in TBCD, encoding the tubulin folding cofactor D. Perturb microtubule dynamics and cause early-onset encephalopathy. *Am J Hum Genet*. 2016;99(4):962-973. doi:10.1016/j.ajhg.2016.08.003
9. Miyake N, Fukai R, Ohba C, et al. Biallelic TBCD mutations cause early-onset neurodegenerative encephalopathy. *Am J Hum Genet*. 2016;99(4):950-961. doi:10.1016/j.ajhg.2016.08.005
10. Tegtmeyer LC, Rust S, van Scherpenzeel M, et al. Multiple phenotypes in phosphoglucomutase 1 deficiency. *N Engl J Med*. 2014;370(6):533-542. doi:10.1056/NEJMoa1206605
11. Abecasis GR, Cherny SS, Cookson WO, Cardon LR. Merlin–rapid analysis of dense genetic maps using sparse gene flow trees. *Nat Genet*. 2002;30(1):97-101. doi:10.1038/ng786
12. Ye J, Coulouris G, Zaretskaya I, Cutcutache I, Rozen S, Madden TL. Primer-BLAST: a tool to design target-specific primers for polymerase chain reaction. *BMC Bioinformatics*. 2012;13:134. doi:10.1186/1471-2105-13-134
13. Choi Y, Sims GE, Murphy S, Miller JR, Chan AP. Predicting the functional effect of amino acid substitutions and indels. *PLOS One*. 2012;7(10):e46688,1-13. doi:10.1371/journal.pone.0046688
14. Landrum MJ, Lee JM, Benson M, et al. Clinvar: improving access to variant interpretations and supporting evidence. *Nucleic Acids Res*. 2018;46(D1):D1062-D1067. doi:10.1093/nar/gkx1153
15. Sim NL, Kumar P, Hu J, Henikoff S, Schneider G, Ng PC. SIFT Web server: predicting effects of amino acid substitutions on proteins. *Nucleic Acids Res*. 2012;40(Web Server issue):W452-W457. doi:10.1093/nar/gks539
16. Schwarz JM, Rodelsperger C, Schuelke M, Seelow D. Mutationtaster evaluates disease-causing potential of sequence alterations. *Nat Methods*. 2010;8:575-576.
17. Zhang Y, Zhang L, Zhou S. Developmental regression and epilepsy of infancy with migrating focal seizures caused by TBCD mutation: a case report and review of the literature. *Neuropediatrics*. 2020;51(1):68-71. doi:10.1055/s-0039-1698423
18. Elmas M, Yıldız H, Erdoğan M, Gogus B, Avcı K, Solak M. Comparison of clinical parameters with whole exome sequencing analysis results of autosomal recessive patients; a center experience. *Mol Biol Rep*. 2019;1:287-299.
19. Tian D, Rizwan K, Liu Y, et al. Biallelic pathogenic variants in TBCD-related neurodevelopment disease with mild clinical features. *Neurol Sci*. 2019;40(11):2325-2331. doi:10.1007/s10072-019-03979-0
20. Di Bella D, Magri S, Benzoni C, et al. Hypomyelinating leukodystrophies in adults: clinical and genetic features. *Eur J Neurol*. 2020;28(3):934-944. doi:10.1111/ene.14646
21. Isik E, Yilmaz S, Atik T, et al. The utility of whole exome sequencing for identification of the molecular etiology in autosomal

recessive developmental and epileptic encephalopathies. *Neurol Sci*. 2020;41(12):3729-3739. doi:10.1007/s10072-020-04619-8
22. Stephen J, Nampoothiri S, Vinayan KP, et al. Cortical atrophy and hypofibrinogenemia due to FGG and TBCD mutations in a single family: a case report. *BMC Med Genet*. 2018;19(1):80. doi:10.1186/s12881-018-0597-6
23. Gronborg S, Risom L, Ek J, et al. A Faroese founder variant in TBCD causes early onset, progressive encephalopathy with a homogenous clinical course. *Eur J Hum Genet*. 2018;26(10):1512-1520. doi:10.1038/s41431-018-0204-5
24. Ikeda T, Nakahara A, Nagano R, et al. TBCD may be a causal gene in progressive neurodegenerative encephalopathy with atypical infantile spinal muscular atrophy. *J Hum Genet*. 2017;4:473-480.
25. Pode-Shakked B, Barash H, Ziv L, et al. Microcephaly, intractable seizures and developmental delay caused by biallelic variants in TBCD: further delineation of a new chaperone-mediated tubulinopathy. *Clin Genet*. May 2017;91(5):725-738. doi:10.1111/cge.12914
26. Edvardson S, Tian G, Cullen H, et al. Infantile neurodegenerative disorder associated with mutations in TBCD, an essential gene in the tubulin heterodimer assembly pathway. *Hum Mol Genet*. 2016;25(2):4635-4648. doi:10.1093/hmg/ddw292
27. Abal M, Andreu JM, Barasoain I. Taxanes: microtubule and centrosome targets, and cell cycle dependent mechanisms of action. *Curr Cancer Drug Targets*. 2003;3(3):193-203. doi:10.2174/1568009033481967
28. Rowinsky EK, Eisenhauer EA, Chaudhry V, Arbuck SG, Donehower RC. Clinical toxicities encountered with paclitaxel (taxol). *Semin Oncol*. 1993;20(4 Suppl 3):1-15.
29. Roosing S, Cremers FPM, Riemslag FCC, et al. A rare form of retinal dystrophy caused by hypomorphic nonsense mutations in CEP290. *Genes*. 2017;8(8).
30. Matthijs G, Souche E, Alders M, et al. Guidelines for diagnostic next-generation sequencing. *Eur J Hum Genet*. 2016;24(1):2-5. doi:10.1038/ejhg.2015.226